European Review for Medical and Pharmacological Sciences 2019; 23: 9000-9008

Targeting miR-106-3p facilitates functional recovery *via* inactivating inflammatory microglia and interfering glial scar component deposition after neural injury

Y.-H. YANG[1], J. ZHU[2]

[1]Department of Spine Section, Baoji Hospital of TCM, Baoji, China
[2]CT/Nuclear Magnetic Chamber, Tongchuan Mining Bureau Center Hospital, Tongchuan, China

Abstract. – OBJECTIVE: The aim of this study was to elucidate whether the knockdown of microRNA-106-3p (miR-106-3p) could mediate the nerve regeneration and functional recovery after the spinal cord injury (SCI) and its potential mechanism.

MATERIALS AND METHODS: Microglia were extracted from the cerebral cortex of the neonatal rats and cultured *in vitro*. Subsequently, biomarkers of M1-type and M2-type in microglia transfected with miR-106-3p inhibitor were measured. Furthermore, *in vivo* SCI model in rats was successfully constructed, and SCI rats were intrathecally injected with miR-106-3p inhibitor or negative control. The expressions of the pro-inflammatory factors in the SCI rats or controls were detected by the enzyme-linked immunosorbent assay (ELISA). The glial scar marker and extracellular matrix were visualized by Western blotting and immunofluorescence, respectively. To observe the nerve function in rats, the movement evaluation was conducted using Basso-Beattie-Bresnahan (BBB) locomotor rating scale.

RESULTS: In the inflammatory microglia, miR-106-3p was markedly up-regulated. Western blotting exhibited the downregulation of M1-type cells and the upregulation of M2-type cells after silencing miR-106-3p. In SCI rats, we discovered that the miR-106-3p level in the injured spinal cord was up-regulated within one week following injury. Meanwhile, the levels of the pro-inflammatory factors were significantly reduced in SCI rats with the miR-106-3p knockdown. At 7 days after the injury, the area of the astrocyte scar in the injured spinal cord was remarkably reduced by *in vivo* knockdown of miR-106-3p. Moreover, the extracellular matrix components secreted in the scar were also significantly inhibited. However, the glial secretion of the neurotrophic factors relatively increased in the SCI rats with the miR-106-3p knockdown. Neurological function recovery was pronounced in SCI rats with the miR-106-3p knockdown relative to controls.

CONCLUSIONS: The silence of miR-106-3p promotes the recovery of the locomotor function and protects the environment of the neurotization by inactivating inflammatory microglia and reducing the scar formation following SCI.

Key Words:
Spinal cord injury (SCI), MiR-106-3p inhibition, Glial scar, Functional recovery.

Introduction

The acute mechanical compression of the spinal cord induces the destruction of the blood-spinal barrier, microvasculature rupture, and neuronal damage, which is called primary spinal cord injury (PSCI)[1]. On the basis of PSCI, the hypoxic tissues, erythrocytes deposition, and damaged cell debris may trigger a cascade of the pathological reactions arranging from the inflammatory response to scar generation. This can eventually contribute to a secondary spinal cord injury (SSCI), where a large number of leukocytes are recruited and the glial cells are activated[2,3]. Microglia are known as a group of immunological macrophages native of the neural tissues. Under normal circumstance, microglia normally guide the normal function of the neural network of the adult central nervous system in a resting state[4-6]. However, the infection and lesion of the neural tissues quickly stimulate microglia activation, which also plays a double-edged role[7]. Type M1 microglia are considered as the pro-inflammatory cells that can secrete reactive oxygen species (ROS), inducible nitric oxide synthase (iNOS), as well as pro-inflammatory factors, including tumor necrosis factor alpha (TNF-α), interleukin-6 (IL-6), and monocyte chemoattractant protein-1

Corresponding Author: Jian Zhu, BM; e-mail: zhujian197606@163.com

(MCP-1)[8-10]. Generally, the cytotoxic effects of type M1 microglia on neurons and oligodendrocytes aggravate neural tissue damage[11]. Compared with M1, the type M2 microglia are granted to phagocytosis of cell debris. Meanwhile, they secrete abundant anti-inflammatory cytokines ranging from IL-10, transforming growth factor β (TGF-β), IL-4, IL-13, and neurotrophic factors[12]. Miron et al[13] have demonstrated that the type M2 microglia promote the proliferation and differentiation of oligodendrocytes and can also be involved in re-myelinization. Therefore, M2 phenotypic microglia exert a neuroprotective role in reducing the inflammatory response and facilitating the nerve repair[14,15]. Besides, the astrocytes surrounding the injured site in the brain transform to reactive astrocytes in response to SCI. The latter further mature into scarring-like astrocytes and eventually accumulate dense glial scars around the injured area[16,17]. These reactive astrocytes are also known as type A1 astrocytes. They do not provide nutritional support and protection for the remaining neurons after injury. Moreover, they cannot possess the phagocytic ability to clean myelin debris[18,19]. Instead, they murder the damaged neurons and oligodendrocytes[20]. Contrarily, the reactive astrocytes express a class of extracellular matrix molecules called chondroitin sulfate proteoglycans (CSPGs), which inhibit the sprouting of neuraxon[21]. In addition, there are many non-neural type cells with various origins, and they possess strong heterogeneity in the blocked lesion area after the inflammatory reaction, including pericytes, fibroblasts from the spinal membrane, and other sources, as well as various immune cells derived from the peripheral blood. This can ruggedize scar structure *via* laminin and fibronectin secretion[22]. Shi et al[23] have demonstrated that the multiple microRNAs (miRNAs) are altered in SCI, serving as critical factors in the pathological mechanism of SCI. For instances, miR-17-5p regulates the reactive astrocyte proliferation in SCI mice[24]. Jin et al[25] have considered that miR-136 controls the apoptosis of neurocytes in spinal cord ischemic injury. Gao et al[26] have indicated that miR-137 inhibits inflammatory response and apoptosis after SCI *via* targeting MK2.

In the current study, we monitored the increase of miR-106-3p in the inflammatory microglia and the inhibitory effect of miR-106-3p in glial inflammation. In the SCI model, we discovered significantly reduced inflammatory factors and reactive astrocytes in the injured site. Fibrous matrixes were down-regulated, while the neurotrophic factors were relatively up-regulated after the knockdown of miR-106-3p. Furthermore, the silence of miR-106-3p ameliorated the chronic inflammation and glial-fibrotic scar formation during the progression of the damage recovering.

Materials and Methods

Primary Microglia Culture and Treatment

To extract primary microglia, the 3-day-old neonatal rats were first sacrificed. Briefly, the cerebral cortex of rats was dissolved in tyrosine solution. After centrifugation, the purified microglia were cultured in Dulbecco's Modified Eagle's Medium (DMEM; Gibco, Rockville, MD, USA) containing 10% fetal bovine serum (FBS; Gibco, Rockville, MD, USA) and 1% streptomycin and penicillin. Until the density of the cell reached 90%, lipopolysaccharide-induced cells (100 ng/mL LPS for 24 h incubation) were transfected with miR-106-3p inhibitor or negative control for 24 h.

Animals and Grouping

A total of 84 male Sprague Dawley (SD) rats (aged at 6 weeks and weighing from 200-220 g) were sacrificed to construct the SCI model. All rats were caged separately, with free access to conventional food and water. The environmental conditions were controlled at 22-24°C, with 50%-65% of humidity and in a 12 h/12 h artificial circadian cycle. All rats were divided into three groups, including: the Sham group, SCI group, and inhibitor group. The rats in the Sham group only received laminectomy. The rats in the SCI group and inhibitor group underwent SCI, and intrathecally injected with normal saline or miR-106-3p inhibitor, respectively. This study was approved by the Animal Ethics Committee of Baoji Hospital of the TCM Animal Center.

Operative Procedure and Treatment

Firstly, rats were anesthetized with 10% paraformaldehyde at a dose of 4 mL/kg and prepared for skin disinfection at the operation area. The SCI procedures were performed as follows: after localization of the spinous process of T10, the skin was cut open, and the fascia muscle tissues were separated to expose the intact T10 lamina. Laminectomy was performed to strip the upper lamina of the spinal cord, followed by a complete expose of the spinal cord. ALLEN bump equipment (10 g

× 5 cm) was then performed to damage the spinal cord tissues. The successful SCI modeling caused spinal cord hemorrhage and delayed the extension of the hind-limbs and tail swing in rats. Next, the rats were intrathecally injected with miR-106-3p inhibitor or normal saline. The incision was sutured, and the skin was sterilized. The auxiliary urination was conducted three times a day until recovery of urination reflex.

Western Blotting

The total protein was extracted from spinal cord tissues or differently treated microglia on ice using a total protein extraction kit containing protease inhibitors and phosphatase inhibitors. After high-speed centrifugation (13000 rpm, 15 minutes) at 4°C, the supernatant fluid was obtained. The protein concentration was determined by the double bicinchoninic acid (BCA) method (Pierce, Rockford, IL, USA). Subsequently, the protein samples were separated by 10% sodium dodecyl sulfate-polyacrylamide gel and transferred onto polyvinylidene difluoride (PVDF) membranes (Millipore, Billerica, MA, USA) at 4°C. Then, the membranes were blocked with 5% non-fatty milk prepared with Tris-Buffered Saline with Tween 20 (TBST) for 1 h at room temperature. After washing 3 times with TBST, the membranes were incubated with primary antibodies (iNOS, Abcam, Cambridge, MA, USA, Rabbit, 1:250; Arg-1, Cell Signaling Technology, Danvers, MA, USA, Rabbit, 1:1000; laminin, Abcam, Cambridge, MA, USA, Rabbit, 1:1000; fibronectin, Abcam, Cambridge, MA, USA, Rabbit, 1:1000; BDNF, Abcam, Cambridge, MA, USA, Rabbit, 1:2000; GAPDH, Proteintech, Rosemont, IL, USA, 1:10000) at 4°C overnight. On the next day, the membranes were incubated with the corresponding secondary antibody (Goat Anti-Rabbit IgG, YiFeiXue Biotechnology, 1:3000, Nanjing, China) at room temperature for 1 h and washed again with TBST for 3 times. Enhanced chemiluminescence (ECL) was used to display the target proteins on an exposure machine.

Quantitative Real Time-Polymerase Chain Reaction (qRT-PCR)

1 mL of TRIzol (Invitrogen, Carlsbad, CA, USA) was added to spinal cord tissues for homogenate. After 5 minutes of incubation at room temperature, the nucleic acid-protein complex was completely separated. For the cells, 0.5 mL of TRIzol was added to cells in each well, followed by incubation on an ice shaker for 10 minutes. 0.2 mL of chloroform was added into tissue/cell lysis corresponding to every 1 mL of TRIzol. The mixture was violently shaken for 15 seconds and incubated at room temperature for 3 minutes. After centrifugation for 15 minutes (10000 RPM, 4°C), the upper water phase was collected, and the isopropyl alcohol was added. The mixture was vibrated and placed at room temperature for 10 minutes. After centrifugation for 10 minutes (10000 RPM, 4°C), RNA precipitation was collected, and the supernatant was discarded. After washing RNA precipitation with 75% ethanol, the mixture was centrifuged (10000 RPM and 4°C) for 5 minutes. The supernatant was discarded, and 30 μL of RNase free water was added to dissolve the extracted RNA. The RNA concentration was measured by Nano Drop to determine the absorbance at 260 nm, 230 nm, and 280 nm. A260/A280 of RNA sample between 1.8 and 2.0, considered to be qualified for qRT-PCR.

The quantitative analysis of mRNA was achieved using Prism 7300 Sequence Detection System (Applied Biosystems, Foster City, CA, USA). 25 μL of the reaction system was prepared, including: 12.5 μL of SYBR Green, 10 mM primers (0.5 mL each from the stock), 10.5 μL of water, and 0.5 μL of the template. The specific PCR conditions were as follows: 10 min denaturation at 95°C; followed by 40 cycles of denaturation at 95°C for 15 s, 60°C annealing for 30 s and 72°C extension for 30 s. U6 was used as an internal reference. The comparative threshold cycle (Ct) method, namely the $2^{-\Delta\Delta Ct}$ method was used to calculate fold amplification. The primer sequences used in this study were as follows: miR-106-3p, F: 5'-GAATGTAGGCATCCTCAACTG-3', R: 5'-GAATCCCGTGTCAAGGAGTA-3'; U6: F: 5'-GCTTCGGCAGCACATATACTAAAAT-3', R: 5'-CGCTTCAGAATTTGCGTGTCAT-3'.

Enzyme-Linked Immunosorbent Assay

The spinal cord samples were first taken from rats and washed in an appropriate amount of Phosphate-Buffered Saline (PBS). Subsequently, the mixture was homogenized and centrifuged for 10 minutes to collect the supernatant. The standard product wells were set on 96-well plates, and the standard products of different concentrations were added successively. The samples were added into the corresponding wells to be tested. Then, the plates were sealed with a sealing film, followed by incubation at room temperature for 30 minutes. Next, the liquid was discarded, and each well was filled with washing solution for

30 seconds (repeated 5 times). Subsequently, the enzyme standard reagent was added into each well, except blank wells. The colorant was added into each well, followed by incubation in the dark for 15 minutes. Next, the termination solution was added to terminate the reaction. The absorbance (OD value) of each well at the wavelength of 450 nm was measured sequentially by zeroing in the blank well. With the concentration of the standard product as the abscissa and OD value as the ordinate, the standard curve was depicted to calculate the concentration of the samples.

Immunofluorescence

The spinal samples were removed from rat spinal columns and placed in 4% paraformaldehyde for 24 h of immobilization. Then, the spinal cords were decalcified and dehydrated under different concentrations of ethanol. After embedded in paraffin, the tissues were cut into sections with a rotary microtome. After de-paraffin treatment, the sections were placed into citrate (PH 6.0) and boiled for 40 minutes. The rabbit serum was utilized to block nonspecific combination at room temperature for 1 h. After washing with PBS, the sections were incubated with primary antibodies (GFAP, Abcam, Rabbit, 1:300; NF 200, Cell Signaling Technology, Danvers, MA, USA, Rabbit, 1:200) at 4°C overnight. After that, the sections were incubated with fluorescent secondary antibodies in the dark for 2 h. After washing, the 4',6-diamidino-2-phenylindole (DAPI) Fluoromount-G was utilized to stain the nucleus and seal the sections for 5 min. Finally, the sections were visualized using a fluorescence microscope.

Behavioral Assessment

Basso-Beattie-Bresnahan (BBB) locomotor rating scale was used to evaluate the recovery of the locomotor coordination function of hindlimbs within four weeks after SCI. The rats were scaled from 0 to 21 based on their movements in an open field in a double-blinded way. The evaluation was conducted at 1, 7, 14, 21, and 28 days after SCI modeling, respectively.

Statistical Analysis

The Statistical Product and Service Solutions (SPSS) 20.0 statistical software (IBM Corp., Armonk, NY, USA) was used for all statistical analyses. The measurement data were expressed as $\chi \pm s$. The *t*-test was used to compare the difference between the two groups. The single-factor analysis of variance (ANOVA) was used for comparison among different groups. The Least Significant Difference (LSD) test or Student-Newman-Keuls (SNK) test was used for pairwise comparison under the condition of homogeneity of variance. All experiments were repeated three times. $p<0.05$ was considered statistically significant.

Results

Targeting Inhibition of MiR-106-3p Reduced Inflammatory Microglia Expression and Regulated Anti-Inflammation In Vitro

At post-SCI, classical type M1 microglia were activated and mediated the inflammatory response in injured tissue sites. Immediately, a large number of inflammatory mediators were released to aggravate cell death in the injured area. However, type M2 microglial exerted the anti-inflammatory and phagocytotic effects, which promoted the recovery and regeneration of the damaged tissues. Here, M1 and M2 biomarkers were detected to estimate the microglia polarization effect influenced by miR-106-3p. We found that miR-106-3p significantly up-regulated in LPS-induced microglia, which was declined in those transfected with miR-106-3p inhibitor (Figure 1A). In addition, the protein level of iNOS was significantly elevated after LPS activation. Arginase-1 (Arg-1), which was considered to be a biomarker of the M2 cells, was lowly expressed. The transfection of miR-106-3p inhibitor showed the opposite tendency on the expressions of iNOS and Arg-1 relative to those with only LPS treatment (Figure 1B). The above results suggested that the inhibition of miR-106-3p was involved in the direction of microglia activation and regulated the glial inflammatory response.

Injection of MiR-106-3p Inhibitor Decreased Expression of Inflammatory Factors by Reducing MiR-106-3p Level

To ascertain the anti-inflammatory effect of miR-106-3p inhibition *in vivo*, we firstly measured miR-106-3p level in rats of the three different treatment groups within one week following SCI. MiR-106-3p level significantly increased in the SCI group, and it was down-regulated in the inhibitor group (Figure 2A). Then, we detected TNF-α, IL-6, and MCP-1 levels in the three groups using ELISA at one-day post-SCI. The results demonstrated that the inhibition of miR-

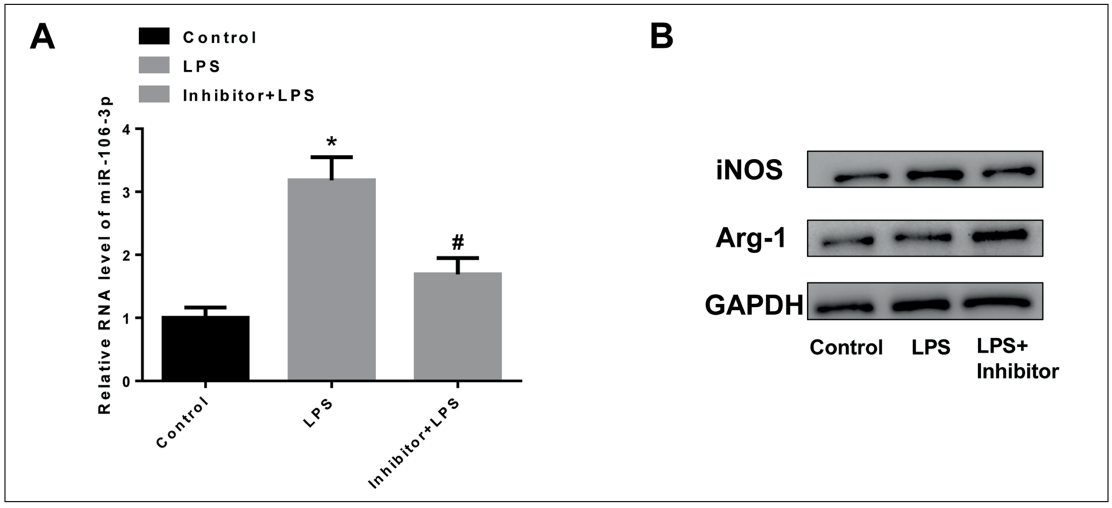

Figure 1. Targeting inhibition of miR-106-3p reduced inflammatory microglia expression and regulated anti-inflammation *in vitro.* **A,** MiR-106-3p alterations in RNA level after microglia untreated, treated with LPS and treated with miR-106-3p inhibitor as well as LPS. **B,** The protein levels of M1 marker-iNOS and M2 marker-Arg-1 in the control group, LPS group, and the inhibitor + LPS group.

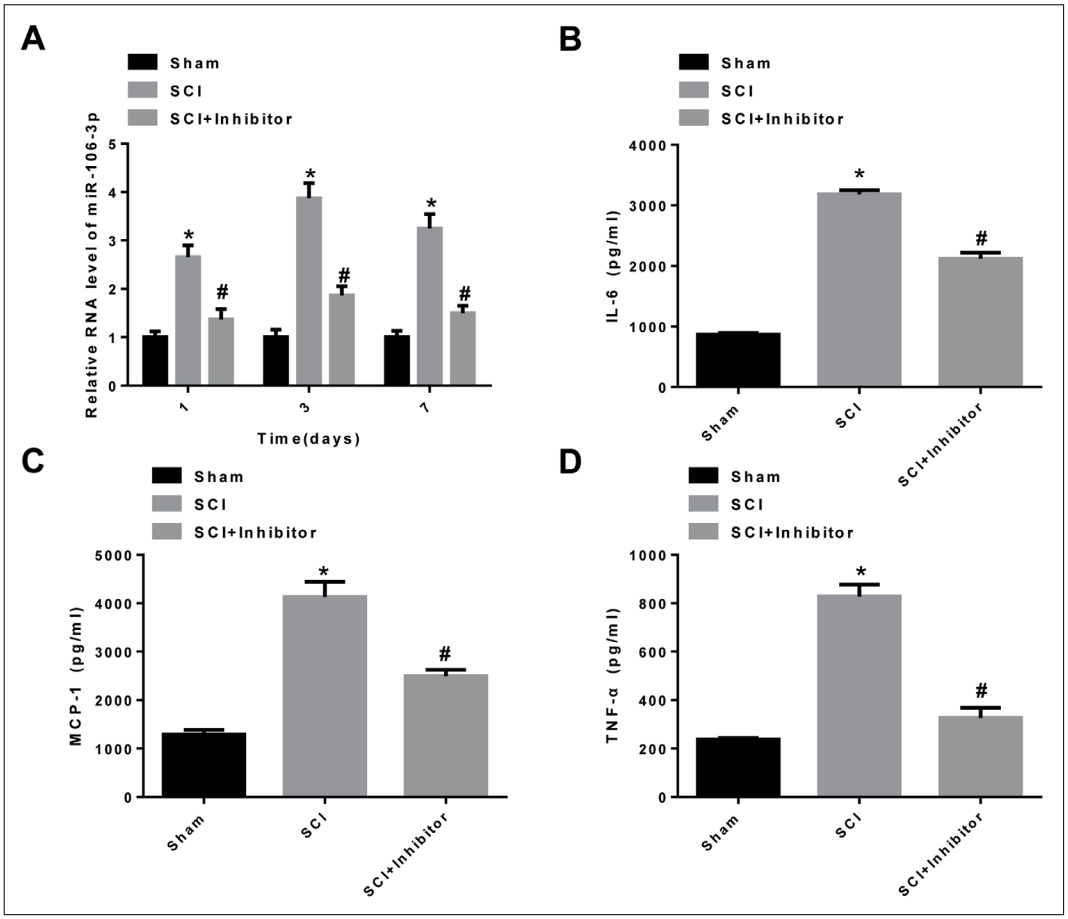

Figure 2. Injection of miR-106-3p inhibitor decreased the expressions of the inflammatory factors by reducing miR-106-3p level. **A,** MiR-106-3p levels in the three groups during one week at post-SCI. **B,** The expressions of IL-6 in the three groups at 1 day following SCI. **C,** MCP-1 in injured spinal cord with different grouping at 1 day after SCI. **D,** TNF-α level at 1 day after SCI detected by ELISA.

106-3p reduced the expressions of the above inflammatory factors (Figures 2B-2D). All the above findings indicated that miR-106-3p inhibitor attenuated the inflammatory response by suppressing miR-106-3p level.

Inhibition of MiR-106-3p Attenuated Glial-Fiber Scar Formation and Facilitated Neural Repair Factor Release

The scar structure following SCI consists of glial cells and fiber compositions, including laminin and fibronectin. The glial-fiber scar is considered as a neural regeneration barrier and can secrete neuro-inhibitory molecules. At the late stage of inflammatory response, the excessive glial scar hinders the repair of the neural structures. Immunofluorescence staining found that the dense glial scar appeared around the damaged area after 7 days following the injury. However, the knockdown of miR-106-3p reduced the area of the glial scar. Meanwhile, the number of neurofilaments was also significantly higher than that of the SCI group (Figure 3A). Furthermore, we detected the proteins levels of laminin, fibronectin, and the glial cell-derived neurotrophic factor (GDNF), which was a neuro-regeneration protein secreted by the glial cells. In the SCI group, laminin and fibronectin were remarkably up-regulated, while GDNF was down-regulated. In SCI rats treated with miR-106-3p inhibitor, we discovered that laminin and fibronectin were remarkably inhibited, whereas GDNF was up-regulated (Figures 3B-3C). All the results suggested that the inhibition of miR-106-3p reduced glial and fibrous scar formation and promoted neural regeneration

.

Treatment of MiR-106-3p Inhibitor Facilitated Locomotor Functional Recovery Following SCI

Finally, we conducted a behavioral experiment at 1, 7, 14, 21, and 28 days following SCI. The performance of the rats in the Sham group was normal throughout the testing period. The locomotor recovery was evaluated in open-field testing using the 21-score BBB locomotor rating scale. The animals suffered paraplegia after SCI and exhibited a low BBB score after 1 day. However, with the continuous recovery of the neural tissues, the early improvement of motor function was showed after 7 days. The rats in the SCI group revealed a moderate recovery, while the rats injected with miR-106-3p inhibitor displayed

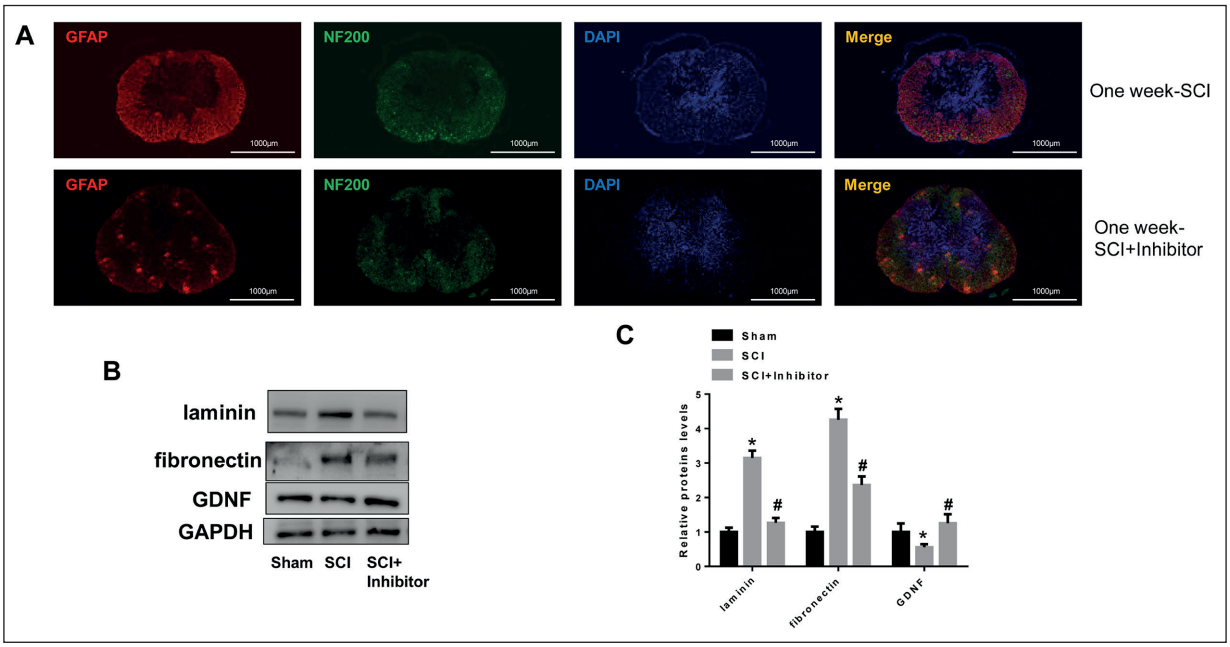

Figure 3. Inhibition of miR-106-3p attenuated glial-fiber scar formation and facilitated the neural repair factor release. **A,** Immunofluorescence co-staining of reactive astrocytes marker (GFAP) and neurofilaments marker NF 200 in injured spinal cord at 7days following SCI (magnification × 20). **B,** The proteins levels of laminin, fibronectin, and GDNF in injured spinal cord at 7 days post-SCI. **C,** The difference among the three groups appeared statistically significant through the Image J software analysis.

significantly better improvement within 4 weeks after SCI (Figure 4). Hence, we concluded that the inhibition of miR-543-5p promoted functional recovery after SCI.

Discussion

After SCI, the injured spinal cord tissues undergo activation and degradation of the inflammatory response[27]. In this pathological process, cell death, hemorrhage, and infiltration of leukocytes in primary lesion may trigger glial inflammation[28]. Subsequently, a large number of activated inflammatory glia release inflammatory factors around the injury, producing formidable microenvironments that are nonviable for neurons[29]. Meanwhile, the inflammatory cytokines can induce apoptosis in damaged neurons rather than dead ones, which also increases the proportion of the neurons loss[30]. Hence, in the polarization of microglia, it represents a critical and effective inflammatory control strategy to reduce the activation ratio of the inflammatory type M1 cells and to increase the number of the anti-inflammatory type M2 cells. Moreover, the formation of the glial scar is attributed to the accumulation of a large number of astrocytes and fiber products. The dense scar structure limits the space regeneration of neuro-filaments and synapse formation. Meanwhile, the exocrine release of a large quantity of the neural inhibitory products worsens the environmental conditions for nerve regeneration[31,32]. The reductions of the size and density of glial scar in the inflammatory regression stage are beneficial to the later neuro-structural remodeling and functional recovery[33]. In the present study, we demonstrated that elevated miR-106-3p level after SCI might mediate the development of various pathological changes. The inhibition of miR-106-3p reduced the activation of inflammatory microglia cells and down-regulated the expressions of the inflammatory factors following SCI. At the late stage of the inflammation, the areas of the glial scar and fiber secretion were significantly reduced. Moreover, the release of the neural growth factor significantly increased, so as to promote nerve regeneration and functional recovery. Although this study failed to find specific targets and signal pathway changes for miR-106-3p-regulated SCI pathological reactions, we demonstrated new strategies in the treatment of SCI by silencing miR-106-3p. Our findings led to the establishment of a more comprehensive SCI treatment system. For what it concerns the unexplored parts, we will continue to reveal the specific mechanism of SCI therapy.

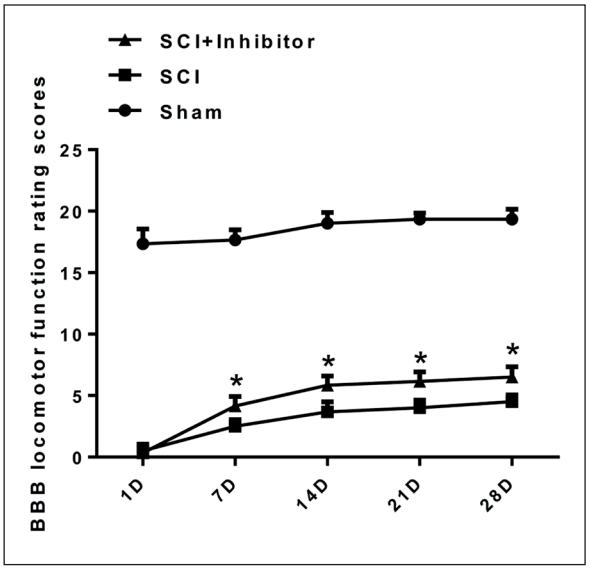

Figure 4. The treatment of miR-106-3p inhibitor facilitated the locomotor functional recovery following SCI. After 7 days after SCI, the difference of the locomotor function between the SCI group and the SCI + Inhibitor group was statistically significant.

Conclusions

We demonstrated that the inhibition of miR-106-3p protected the neuro-mechanisms and improved the functional recovery by polarizing the inflammatory glial cell population and relieving glial fibrous scar area after SCI.

Conflict of Interest

The Authors declare that they have no conflict of interests.

References

1) Muradov JM, Hagg T. Intravenous infusion of magnesium chloride improves epicenter blood flow during the acute stage of contusive spinal cord injury in rats. J Neurotrauma 2013; 30: 840-852.

2) Lin CA, Duan KY, Wang XW, Zhang ZS. MicroRNA-409 promotes recovery of spinal cord injury by regulating ZNF366. Eur Rev Med Pharmacol Sci 2018; 22: 3649-3655.

3) Kanno H, Ozawa H, Sekiguchi A, Yamaya S, Itoi E. Induction of autophagy and autophagic cell death in damaged neural tissue after acute spinal cord injury in mice. Spine (Phila Pa 1976) 2011; 36: E1427-E1434.

4) Epelman S, Lavine KJ, Randolph GJ. Origin and functions of tissue macrophages. Immunity 2014; 41: 21-35.

5) Erny D, Hrabe DAA, Jaitin D, Wieghofer P, Staszewski O, David E, Keren-Shaul H, Mahlakoiv T, Jakobshagen K, Buch T, Schwierzeck V, Utermohlen O, Chun E, Garrett WS, McCoy KD, Diefenbach A, Staeheli P, Stecher B, Amit I, Prinz M. Host microbiota constantly control maturation and function of microglia in the CNS. Nat Neurosci 2015; 18: 965-977.

6) Michell-Robinson MA, Touil H, Healy LM, Owen DR, Durafourt BA, Bar-Or A, Antel JP, Moore CS. Roles of microglia in brain development, tissue maintenance and repair. Brain 2015; 138: 1138-1159.

7) Schmitt AB, Buss A, Breuer S, Brook GA, Pech K, Martin D, Schoenen J, Noth J, Love S, Schroder JM, Kreutzberg GW, Nacimiento W. Major histocompatibility complex class II expression by activated microglia caudal to lesions of descending tracts in the human spinal cord is not associated with a T cell response. Acta Neuropathol 2000; 100: 528-536.

8) Park J, Min JS, Kim B, Chae UB, Yun JW, Choi MS, Kong IK, Chang KT, Lee DS. Mitochondrial ROS govern the LPS-induced pro-inflammatory response in microglia cells by regulating MAPK and NF- κB pathways. Neurosci Lett 2015; 584: 191-196.

9) Park SY, Park SJ, Park TG, Rajasekar S, Lee SJ, Choi YW. Schizandrin C exerts anti-neuroinflammatory effects by upregulating phase II detoxifying/antioxidant enzymes in microglia. Int Immunopharmacol 2013; 17: 415-426.

10) Chantong B, Kratschmar DV, Lister A, Odermatt A. Dibutyltin promotes oxidative stress and increases inflammatory mediators in BV-2 microglia cells. Toxicol Lett 2014; 230: 177-187.

11) Genis P, Jett M, Bernton EW, Boyle T, Gelbard HA, Dzenko K, Keane RW, Resnick L, Mizrachi Y, Volsky DJ, Et A. Cytokines and arachidonic metabolites produced during human immunodeficiency virus (HIV)-infected macrophage-astroglia interactions: implications for the neuropathogenesis of HIV disease. J Exp Med 1992; 176: 1703-1718.

12) Chan A, Magnus T, Gold R. Phagocytosis of apoptotic inflammatory cells by microglia and modulation by different cytokines: mechanism for removal of apoptotic cells in the inflamed nervous system. Glia 2001; 33: 87-95.

13) Miron VE, Boyd A, Zhao JW, Yuen TJ, Ruckh JM, Shadrach JL, van Wijngaarden P, Wagers AJ, Williams A, Franklin R, Ffrench-Constant C. M2 microglia and macrophages drive oligodendrocyte differentiation during CNS remyelination. Nat Neurosci 2013; 16: 1211-1218.

14) Tang Y, Le W. Differential roles of M1 and M2 microglia in neurodegenerative diseases. Mol Neurobiol 2016; 53: 1181-1194.

15) Crain JM, Nikodemova M, Watters JJ. Microglia express distinct M1 and M2 phenotypic markers in the postnatal and adult central nervous system in male and female mice. J Neurosci Res 2013; 91: 1143-1151.

16) Codeluppi S, Svensson CI, Hefferan MP, Valencia F, Silldorff MD, Oshiro M, Marsala M, Pasquale EB. The Rheb-mTOR pathway is upregulated in reactive astrocytes of the injured spinal cord. J Neurosci 2009; 29: 1093-1104.

17) Myer DJ, Gurkoff GG, Lee SM, Hovda DA, Sofroniew MV. Essential protective roles of reactive astrocytes in traumatic brain injury. Brain 2006; 129: 2761-2772.

18) Li S, Uno Y, Rudolph U, Cobb J, Liu J, Anderson T, Levy D, Balu DT, Coyle JT. Astrocytes in primary cultures express serine racemase, synthesize d-serine and acquire A1 reactive astrocyte features. Biochem Pharmacol 2018; 151: 245-251.

19) Vermeiren C, Najimi M, Vanhoutte N, Tilleux S, de Hemptinne I, Maloteaux JM, Hermans E. Acute up-regulation of glutamate uptake mediated by mGluR5a in reactive astrocytes. J Neurochem 2005; 94: 405-416.

20) Liddelow SA, Guttenplan KA, Clarke LE, Bennett FC, Bohlen CJ, Schirmer L, Bennett ML, Munch AE, Chung WS, Peterson TC, Wilton DK, Frouin A, Napier BA, Panicker N, Kumar M, Buckwalter MS, Rowitch DH, Dawson VL, Dawson TM, Stevens B, Barres BA. Neurotoxic reactive astrocytes are induced by activated microglia. Nature 2017; 541: 481-487.

21) Cua RC, Lau LW, Keough MB, Midha R, Apte SS, Yong VW. Overcoming neurite-inhibitory chondroitin sulfate proteoglycans in the astrocyte matrix. Glia 2013; 61: 972-984.

22) Skold M, Cullheim S, Hammarberg H, Piehl F, Suneson A, Lake S, Sjogren A, Walum E, Risling M. Induction of VEGF and VEGF receptors in the spinal cord after mechanical spinal injury and prostaglandin administration. Eur J Neurosci 2000; 12: 3675-3686.

23) Shi Z, Zhou H, Lu L, Li X, Fu Z, Liu J, Kang Y, Wei Z, Pan B, Liu L, Kong X, Feng S. The roles of microRNAs in spinal cord injury. Int J Neurosci 2017; 127: 1104-1115.

24) Hong P, Jiang M, Li H. Functional requirement of dicer1 and miR-17-5p in reactive astrocyte proliferation after spinal cord injury in the mouse. Glia 2014; 62: 2044-2060.

25) Jin R, Xu S, Lin X, Shen M. MiR-136 controls neurocytes apoptosis by regulating tissue inhibitor of metalloproteinases-3 in spinal cord ischemic injury. Biomed Pharmacother 2017; 94: 47-54.

26) Gao L, Dai C, Feng Z, Zhang L, Zhang Z. MiR-137 inhibited inflammatory response and apoptosis after spinal cord injury via targeting of MK2. J Cell Biochem 2018; 119: 3280-3292.

27) Tian DS, Xie MJ, Yu ZY, Zhang Q, Wang YH, Chen B, Chen C, Wang W. Cell cycle inhibition attenuates microglia induced inflammatory response and alleviates neuronal cell death after spinal cord injury in rats. Brain Res 2007; 1135: 177-185.

28) Wang X, Cao K, Sun X, Chen Y, Duan Z, Sun L, Guo L, Bai P, Sun D, Fan J, He X, Young W, Ren Y. Macrophages in spinal cord injury: phenotypic and functional change from exposure to myelin debris. Glia 2015; 63: 635-651.

29) Donnelly DJ, Longbrake EE, Shawler TM, Kigerl KA, Lai W, Tovar CA, Ransohoff RM, Popovich PG. Deficient CX3CR1 signaling promotes recovery after mouse spinal cord injury by limiting the recruitment and activation of Ly6Clo/iNOS+ macrophages. J Neurosci 2011; 31: 9910-9922.

30) Kaur C, Sivakumar V, Zou Z, Ling EA. Microglia-derived proinflammatory cytokines tumor necrosis factor-alpha and interleukin-1beta induce Purkinje neuronal apoptosis via their receptors in hypoxic neonatal rat brain. Brain Struct Funct 2014; 219: 151-170.

31) Alonso G. NG2 proteoglycan-expressing cells of the adult rat brain: possible involvement in the formation of glial scar astrocytes following stab wound. Glia 2005; 49: 318-338.

32) Wanner IB, Anderson MA, Song B, Levine J, Fernandez A, Gray-Thompson Z, Ao Y, Sofroniew MV. Glial scar borders are formed by newly proliferated, elongated astrocytes that interact to corral inflammatory and fibrotic cells via STAT3-dependent mechanisms after spinal cord injury. J Neurosci 2013; 33: 12870-12886.

33) McKeon RJ, Schreiber RC, Rudge JS, Silver J. Reduction of neurite outgrowth in a model of glial scarring following CNS injury is correlated with the expression of inhibitory molecules on reactive astrocytes. J Neurosci 1991; 11: 3398-3411.